Supplementary Information

Effect of buffer/iodide electrolyte on electrochemical capacitor performance

Amelia Klimek, Maciej Tobis, Elzbieta Frackowiak*

Institute of Chemistry and Technical Electrochemistry, Poznan University of Technology,

Berdychowo 4, Poznan 60-965, Poland

*Corresponding author

elzbieta.frackowiak@put.poznan.pl

Table S1 Specific surface area and pore volume of micro/mesoporous carbons: Kynol 5092-20 and salt templated C-ST.

	S_{BET} ($m^2\ g^{-1}$)	V_{micro} ($cm^3\ g^{-1}$)	V_{meso} ($cm^3\ g^{-1}$)
Kynol 5092-20	2100	0.80	0.05
C-ST	2640	0.97	0.16

Table S2 Diameters of selected solvated ions: Na^+, I^-, HPO_4^{2-}, CH_3COO^-, $C_3H_4(OH)(COO)_3^{3-}$ [46-49]

Ion	**Solvated ion diameter (nm)**
Na^+	0.486
I^-	0.600
HPO_4^{2-}	0.604
CH_3COO^-	0.706
$C_3H_4(OH)(COO)_3^{3-}$	1.099

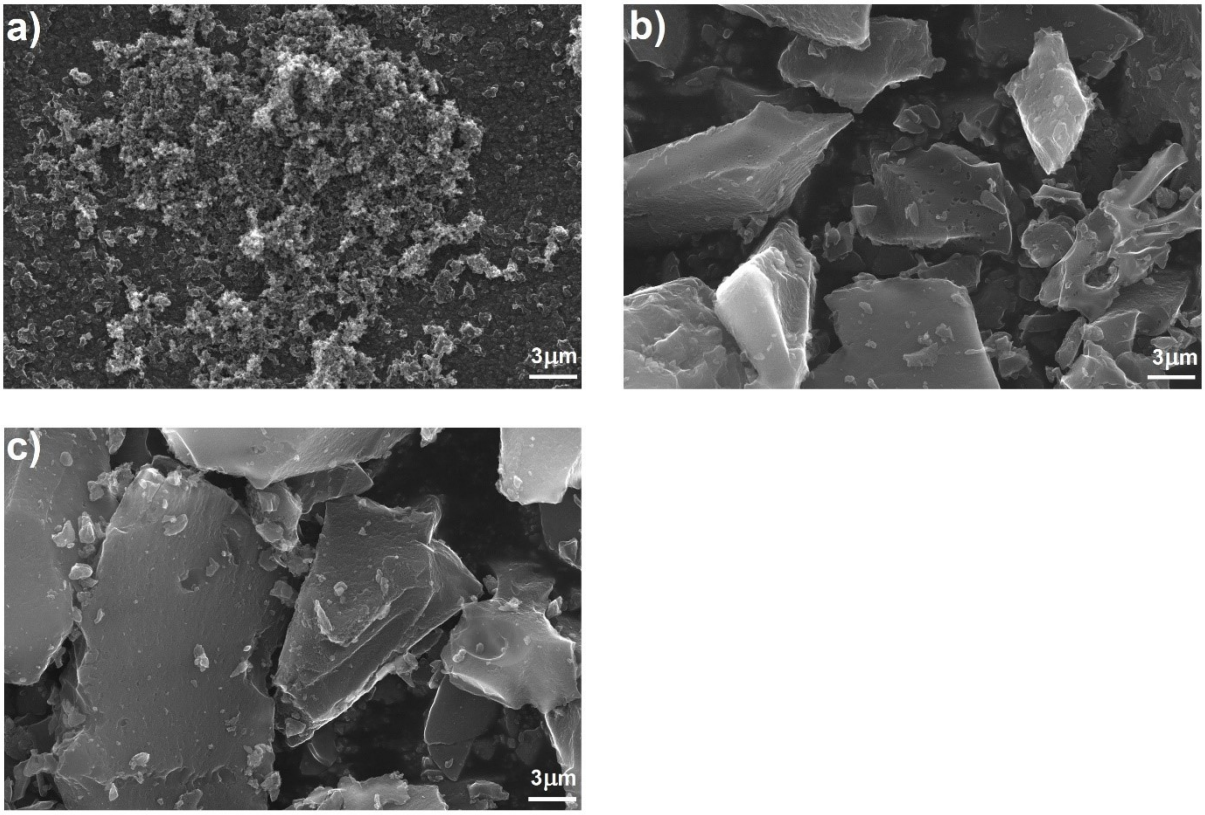

Fig. S1 SEM images of **a)** BP2000 activated carbon; **b)** YP80F activated carbon; **c)** YP50F activated carbon.

Table S3 Conductivity (mS cm^{-1}) and pH measurements of sodium iodide (0.2 mol L^{-1}) and acetate buffer (AcB), citrate buffer (CB), phosphate buffer (PhB) with/without additive of sodium iodide (0.2, 0.5, 1, 2 mol L^{-1}).

Electrolyte	Conductivity (mS cm^{-1})	pH
0.2 mol L^{-1} NaI	20.4	8.5
AcB	63.3	5.08
AcB + 0.2 mol L^{-1} NaI	72.2	5.05
AcB + 0.5 mol L^{-1} NaI	84.5	5.24
AcB + 1 mol L^{-1} NaI	102.4	4.94
AcB + 2 mol L^{-1} NaI	132.4	4.94
CB	3.0	3.74
CB + 0.2 mol L^{-1} NaI	16.5	3.58
CB + 0.5 mol L^{-1} NaI	41.2	3.48
CB + 1 mol L^{-1} NaI	89.0	3.30
CB + 2 mol L^{-1} NaI	76.0	3.25
PhB	6.95	7.18
PhB + 0.2 mol L^{-1} NaI	25.5	6.98
PhB + 0.5 mol L^{-1} NaI	51.9	6.77
PhB + 1 mol L^{-1} NaI	92.1	6.55
PhB + 2 mol L^{-1} NaI	154.7	6.24

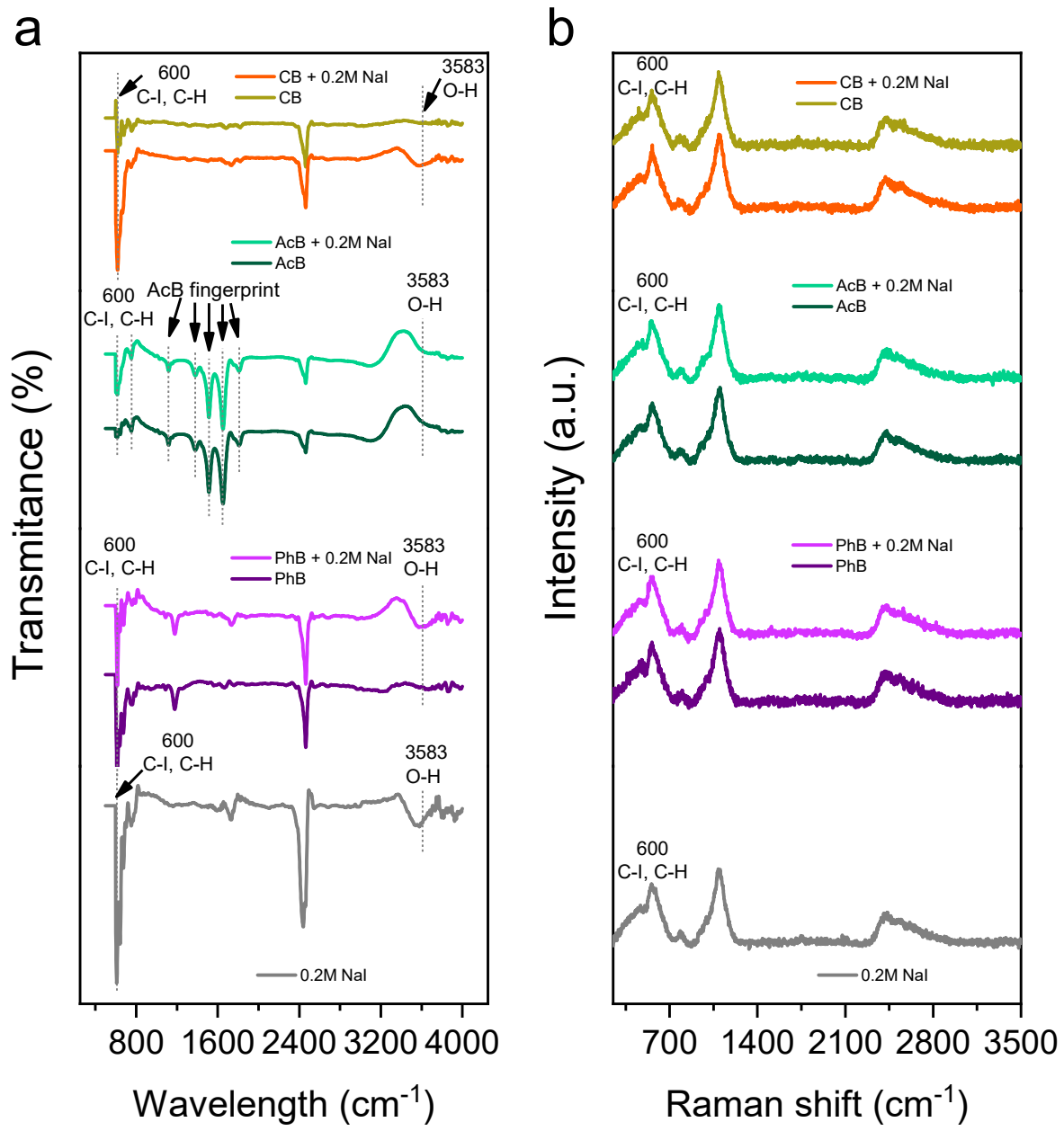

Fig. S2 a) FT-IR and **b)** Raman spectra for the electrolyte solutions with indicated stretching and vibrational modes.

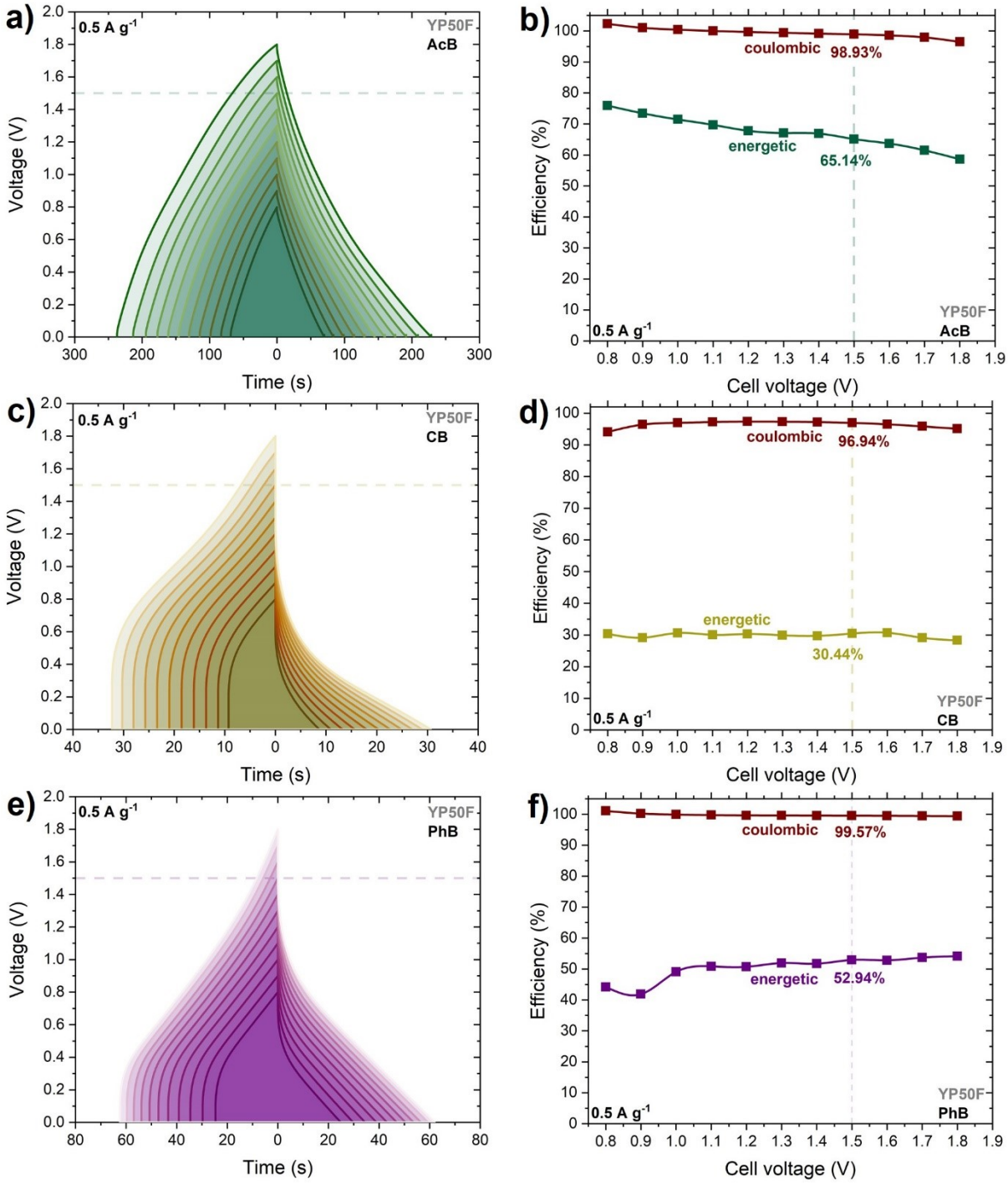

Fig. S3 Galvanostatic charge/discharge voltage extension at 0.5 A g^{-1} for EC operating in **a)** acetate buffer; **c)** citrate buffer; **e)** phosphate buffer for various voltages. Energetic and coulombic efficiency calculated from GCD curves for EC operating in **b)** acetate buffer; **d)** citrate buffer; **f)** phosphate buffer.

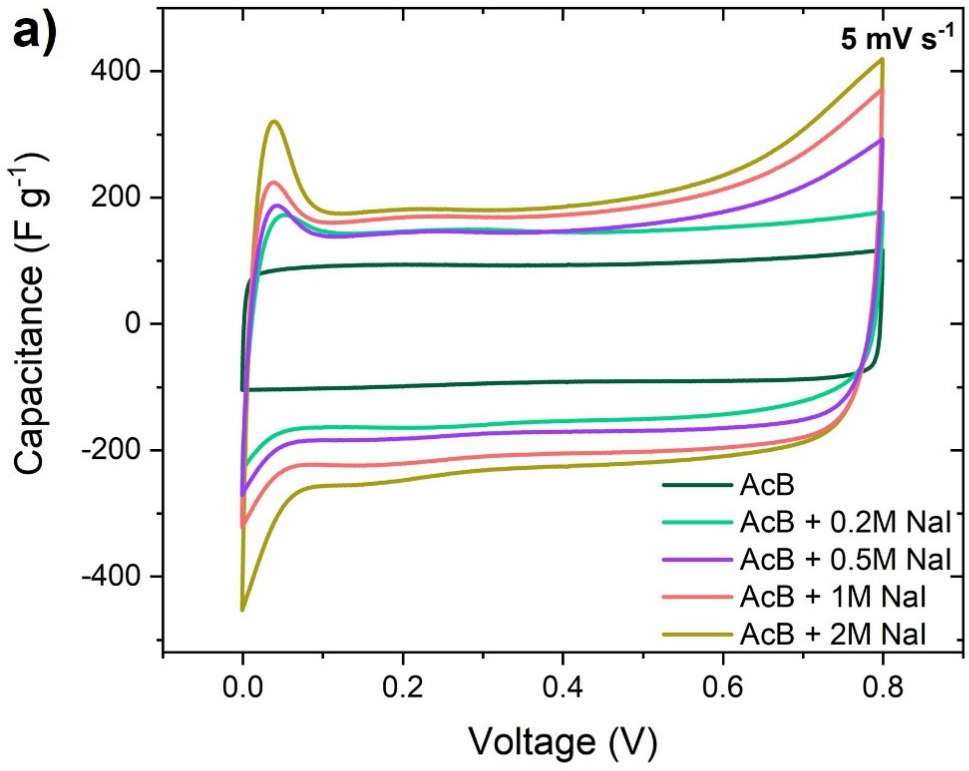

Fig. S4 Cyclic voltammograms recorded at 5 mV s^{-1} for ECs based on YP50F operating in acetate buffer without and with NaI additive of several concentrations (0.2, 0.5, 1, 2 mol L^{-1}).

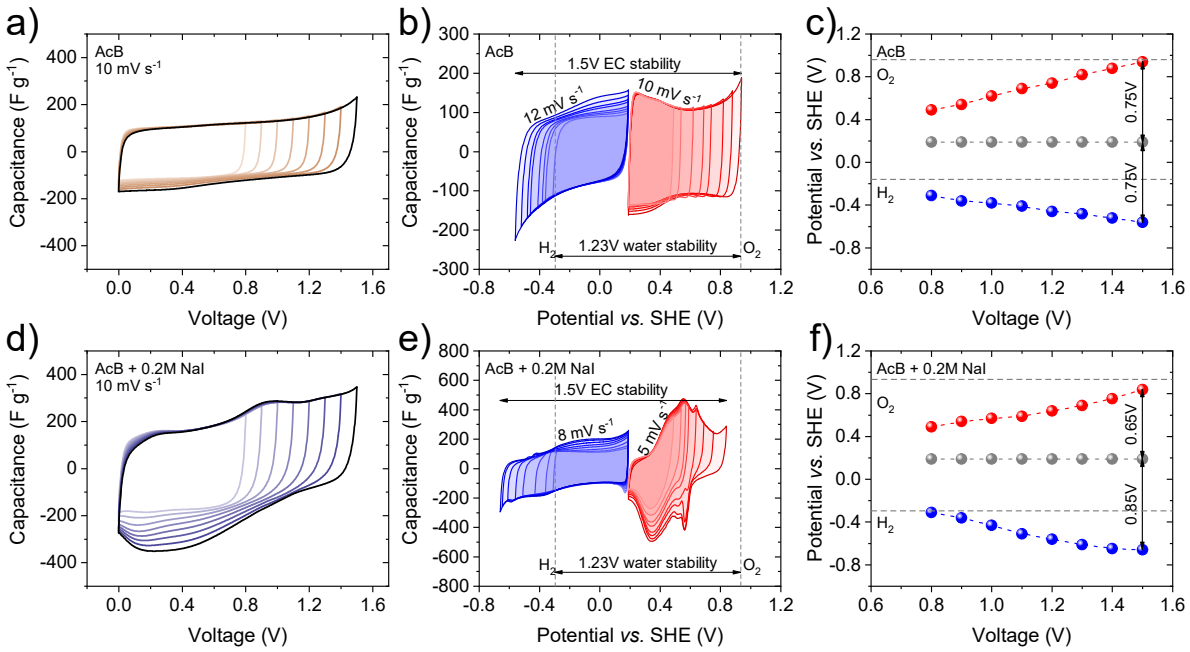

Fig. S5 Electrochemical studies of three-electrode Swagelok cell with reference while monitoring the potential of positive and negative electrode operating in different electrolytes. Cyclic voltammograms of cells operating in AcB and AcB + 0.2 mol L^{-1} NaI **a), d)**. Electrochemical behavior of electrodes during CV measurements **b), e)**. Cut-off potential range for positive and negative electrodes **c), f)**.

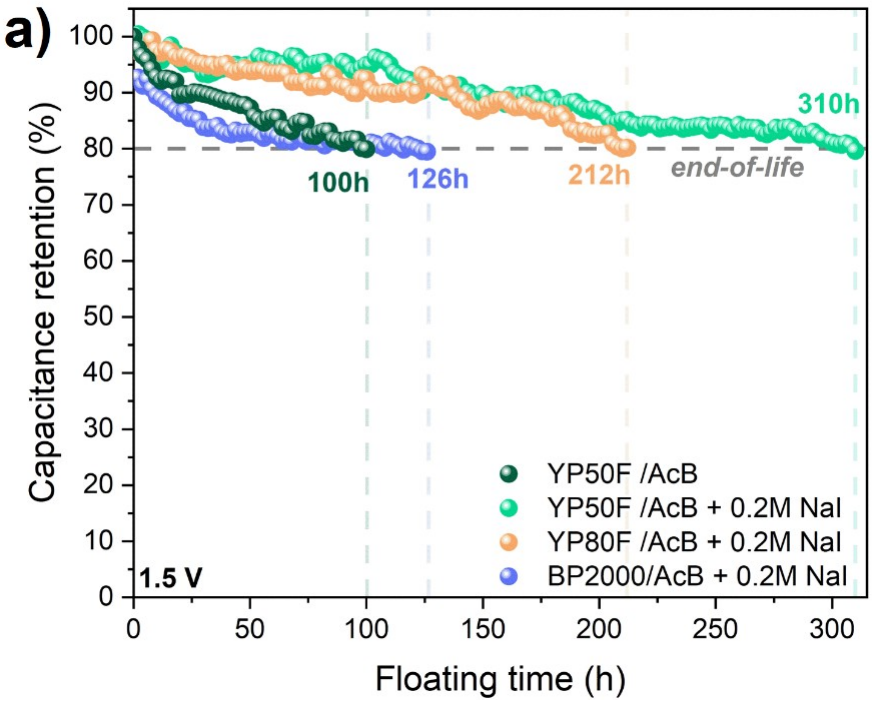

Fig. S6 a) Capacitance retention of different carbons micro/mesoporous carbons (YP50F, YP80F, BP2000) based ECs operating in acetate buffer with/without 0.2 mol L^{-1} NaI additive during floating (at 1.5 V).

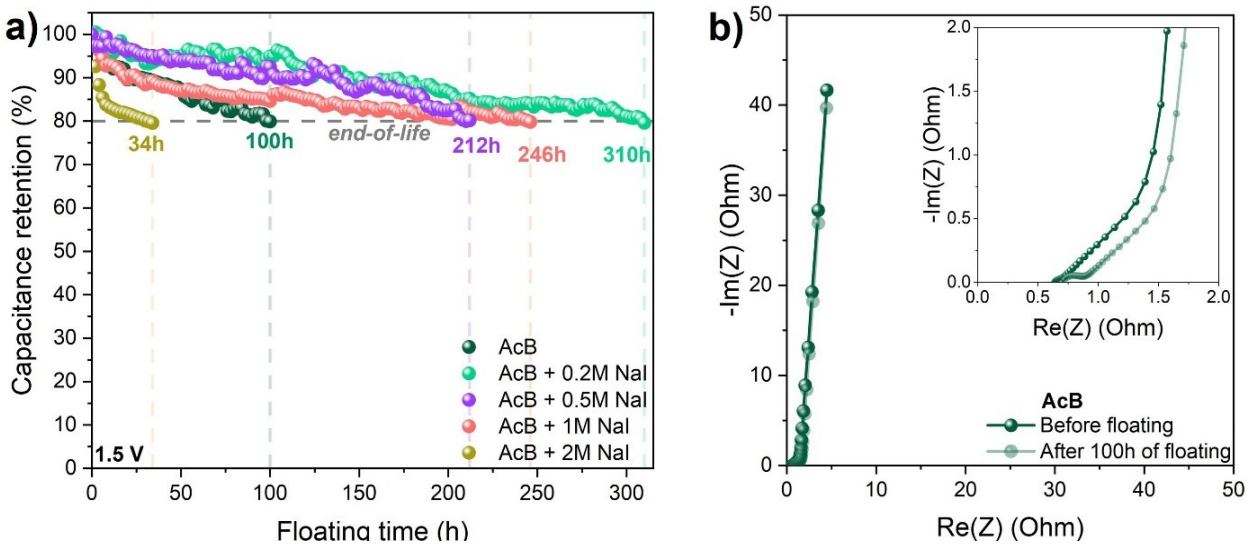

Fig. S7 a) Capacitance retention of YP50F based ECs operating in acetate buffer with/without 0.2, 0.5, 1, and 2 mol L^{-1} NaI additive during floating (at 1.5 V); **b)** Nyquist plots obtained for YP50F based ECs operating in acetate buffer before and after 100 h of floating.

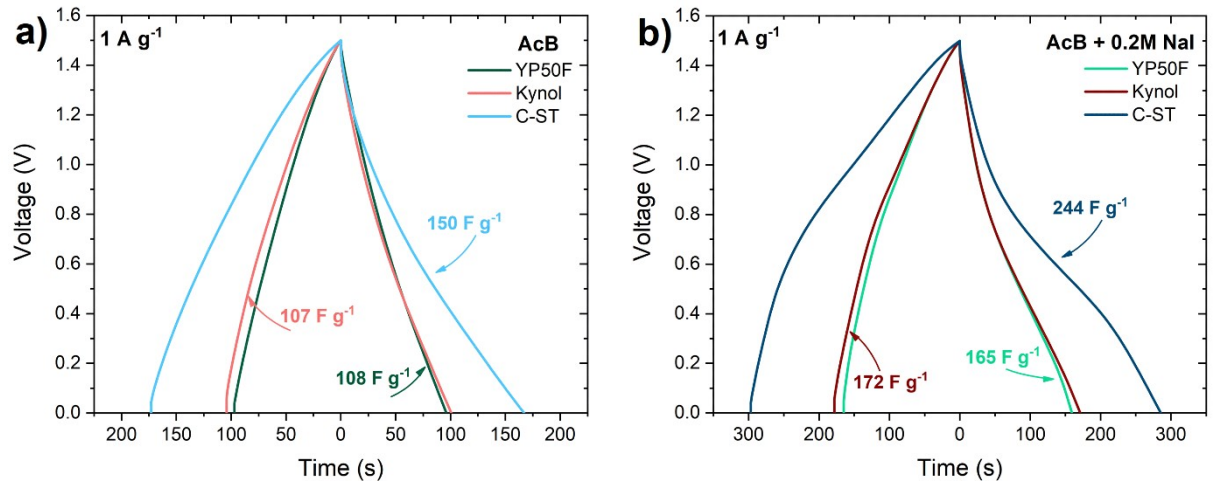

Fig. S8 Galvanostatic charge/discharge profiles recorded at 1 A g^{-1} for ECs based on YP50F, Kynol and C-ST carbons operating in **a)** acetate buffer; **b)** acetate buffer + 0.2 mol L^{-1} NaI.

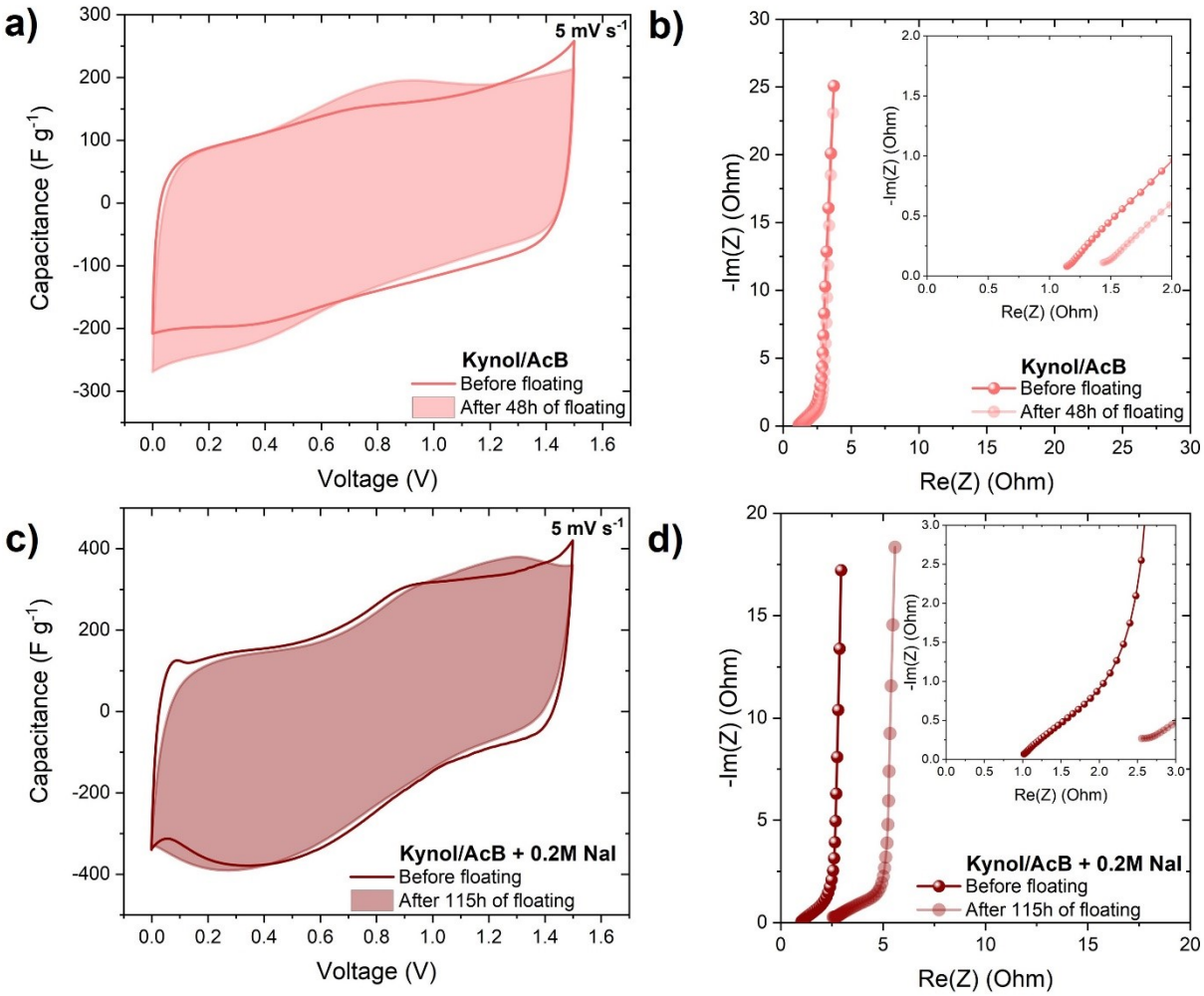

Fig. S9 Cyclic voltammogram at 5 mV s^{-1} recorded for EC based on Kynol operating in **a)** acetate buffer before and after 48 h floating; **c)** acetate buffer + 0.2 mol L^{-1} NaI before and after 115 h floating. Nyquist plots obtained for Kynol based ECs operating in **b)** acetate buffer before and after 48 h of floating and **d)** acetate buffer + 0.2 mol L^{-1} NaI before and after 115 h floating.

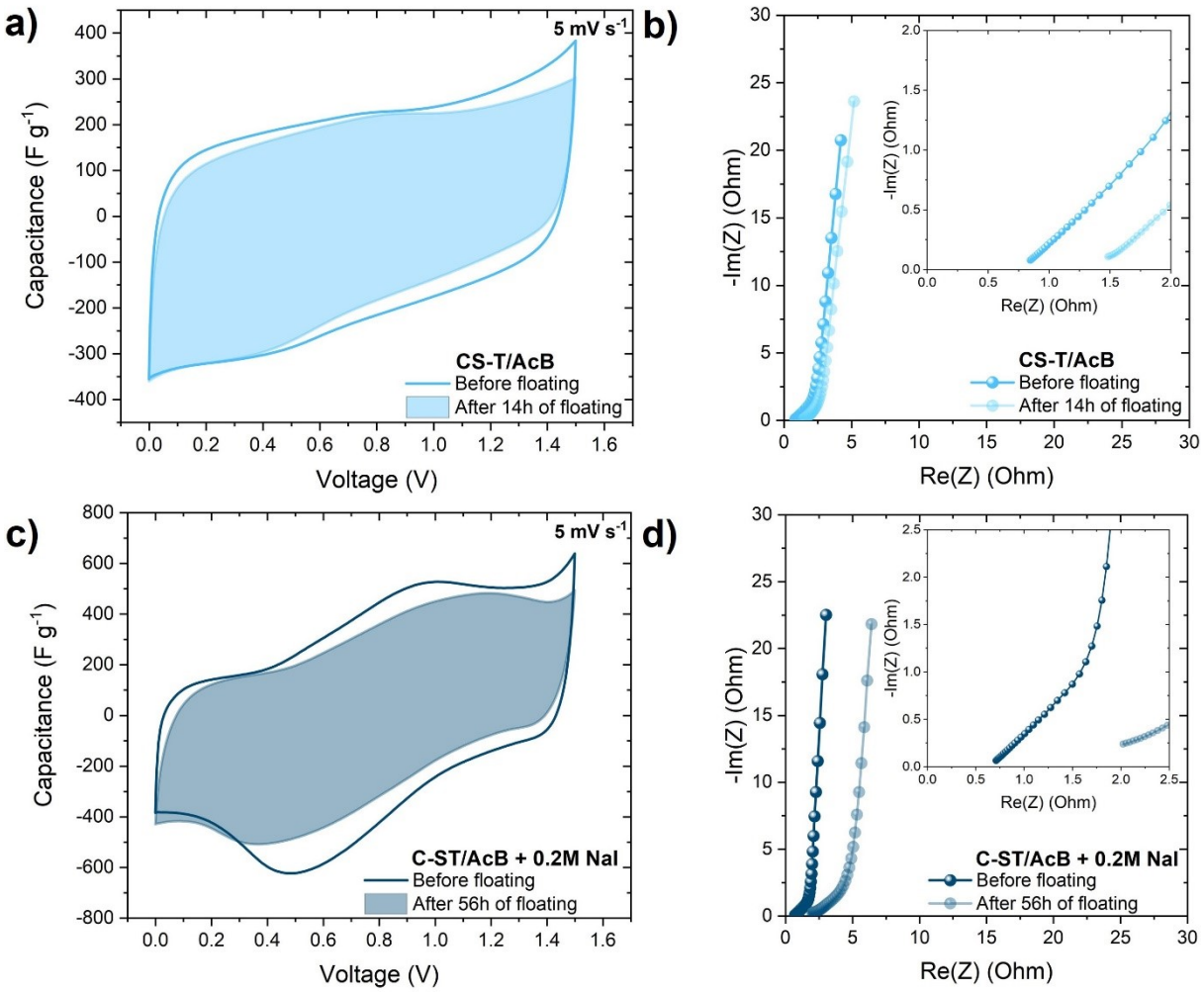

Fig. S10 Cyclic voltammogram at 5 mV s^{-1} recorded for EC based on C-ST operating in **a)** acetate buffer before and after 48 h floating; **c)** acetate buffer + 0.2 mol L^{-1} NaI before and after 115 h floating; Nyquist plots obtained for C-ST based ECs operating in **b)** acetate buffer before and after 48 h of floating and **d)** acetate buffer + 0.2 mol L^{-1} NaI before and after 115 h floating.

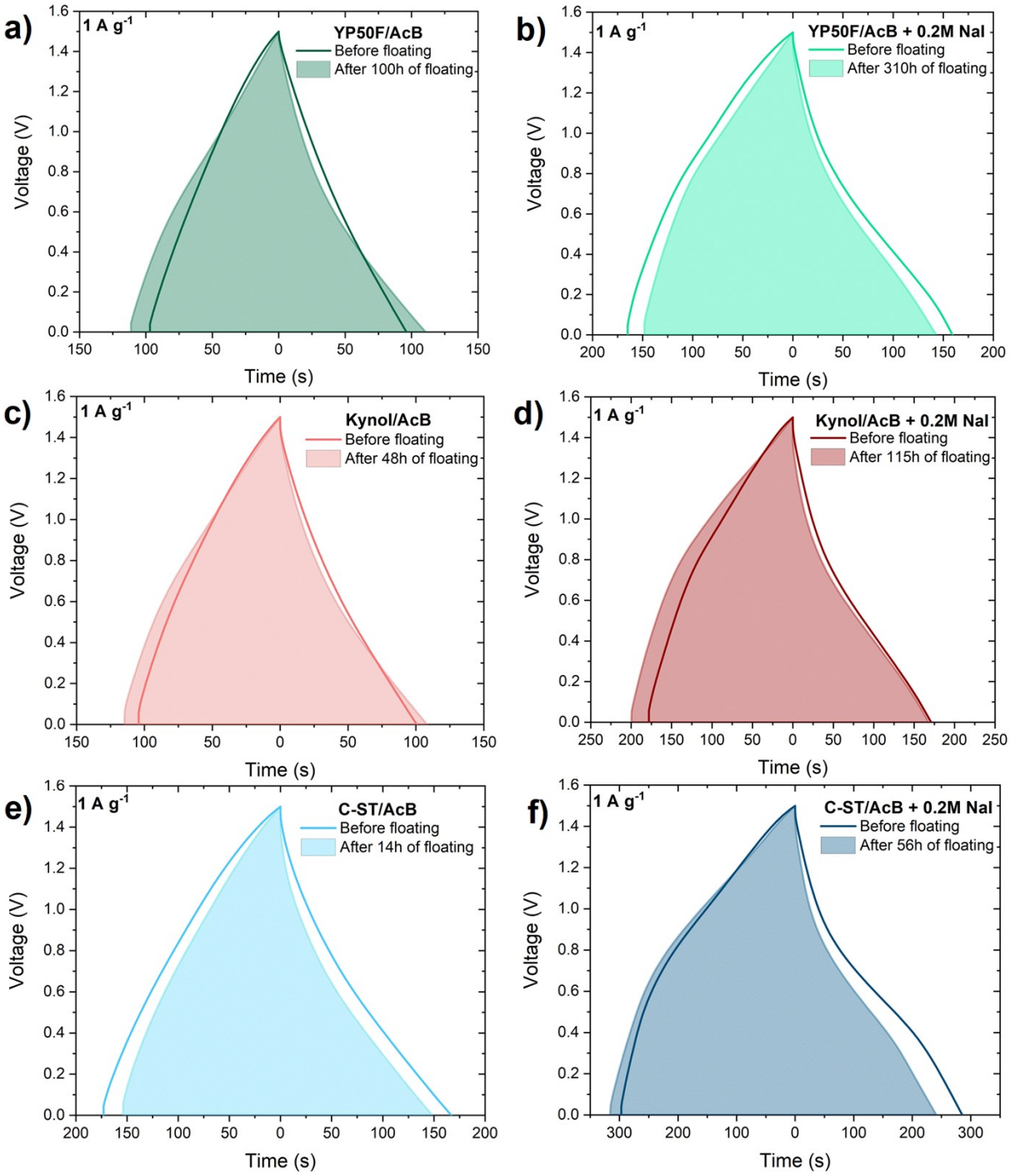

Fig. S11 Galvanostatic charge/discharge profiles before and after floating for ECs based on **a)** YP50F activated carbon operating in acetate buffer; **b)** YP50F activated carbon operating in acetate buffer + 0.2 mol L^{-1} NaI; **c)** Kynol carbon cloth operating in acetate buffer; **d)** Kynol carbon cloth operating in acetate buffer + 0.2 mol L^{-1} NaI; **e)** C-ST activated carbon operating in acetate buffer; **f)** C-ST activated carbon operating in acetate buffer + 0.2 mol L^{-1} NaI.

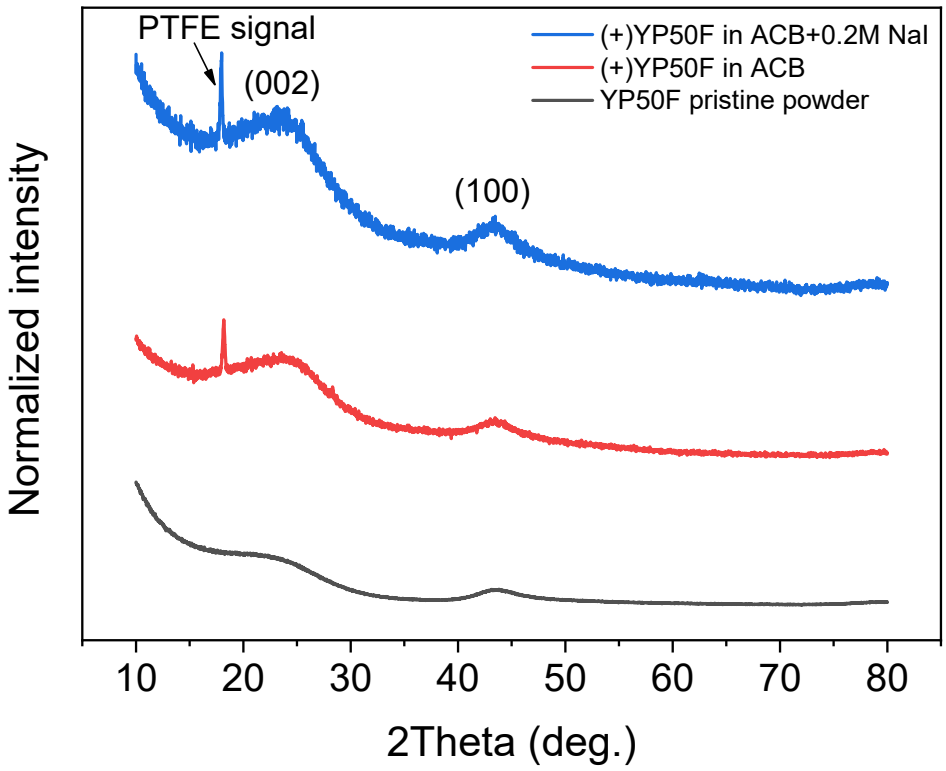

Fig. S12 X-ray diffraction patterns (XRD) of pristine YP50F powder and positive electrodes after floating tests conducted in AcB and AcB + 0.2 mol L^{-1} NaI.

Table S4. Surface composition (atomic %) determined by fitting XPS spectra for electrodes after aging in different electrolytes.

	C						O		I	
Binding energy [eV]	284.4	285.0	286.3	287.6	288.9	290.3	532.2	533.8	618.4	620.6
Compound / Oxidation State	C=C sp^2	C-C sp^3	C-O-C, C-OH	C=O, O-C-O	O-C=O	-COOH	O-Si, O=C, C-O-C	C-O, -OH	NaI	CH-I
Pristine YP50F	56.9	10.4	7.0	3.2	2.6	2.7	7.7	2.2	0.0	0.0
AcB (-)	51.6	11.8	6.1	3.1	2.6	1.9	10.6	0.8	0.0	0.0
AcB (+)	41.4	12.2	6.3	3.8	3.7	2.2	6.8	4.9	0.0	0.0
AcB+0.2M NaI (-)	51.2	12.5	5.7	2.7	2.7	2.2	8.0	1.9	0.05	0.02
AcB+0.2M NaI (+)	47.0	10.8	6.6	3.8	2.8	1.7	8.3	3.3	0.16	0.11

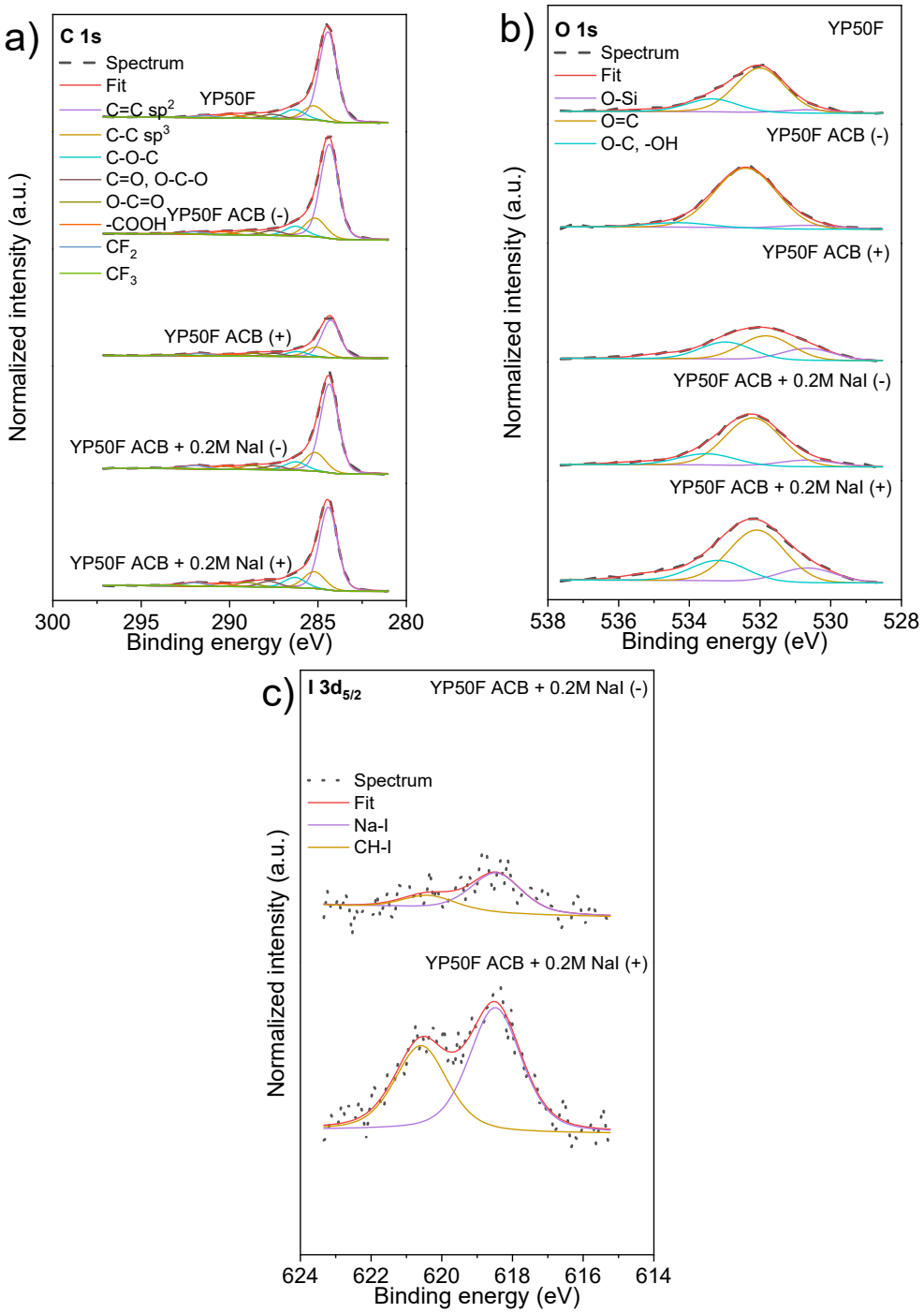

Fig. S13. X-ray photoelectron spectroscopy of a) C 1s region, b) O 1s region, and c) I $3d_{5/2}$ region for pristine, positive and negative YP50F electrodes after floating in different electrolytes with and without addition of iodides.